VIP

Live-Cell dSTORM of Cellular DNA Based on Direct DNA Labeling

Alexander Benke and Suliana Manley*[a]

Super-resolution (SR) fluorescence imaging[1–4] relies on specially adapted microscopes and analysis software, but equally important are the fluorescent probes used to label biological proteins and molecules of interest. In point-localization SR, the on and off rates of fluorophore photoswitching must be controlled to separate the signals from individual molecules temporally. The fluorescence from each molecule is then spatially localized;[5] this allows their positions to be obtained with nanometer precision.[6] Molecular positions are then rendered to give a reconstructed image with a spatial resolution of up to several tens of nanometers.[7, 8] Although fluorescent proteins can be used as labels,[9] synthetic dyes have the advantage of higher photon yields that lead to higher attainable resolution.[10] A special challenge for chemical biologists is to develop or identify synthetic dyes that are compatible with live-cell SR imaging as most dyes are not cell membrane-permeable. Recently, the point-localization SR method of direct stochastic optical reconstruction microscopy (dSTORM)[3, 11] was used to image histone H2B proteins in living cells.[12, 13] Proteins were labeled with rhodamine and oxazaline dyes by using the genetically encoded chemical trimethoprim[14] or SNAP[15] tags. In a separate study, dSTORM was applied in vitro to image purified DNA by direct labeling with the cyanine-based YoYo-1 dye.[16] However, most DNA-associating dyes are not compatible with live-cell imaging owing to their cell impermeability and cytotoxicity. Thus, live-cell super-resolution imaging of DNA structure has never been demonstrated.

We present here the imaging of DNA in living cells with dSTORM based on direct labeling with the commercially available cyanine-based Picogreen dye. Picogreen has several advantages over other DNA-specific dyes for live-cell imaging, including minimal perturbation to DNA structure and an increase in fluorescence upon binding that results in low background fluorescence. We identified a live-cell imaging medium that optimizes the reversible photoswitching of the fluorophores, and used it to resolve nuclear and mitochondrial DNA structure directly. Furthermore, due to the excellent preservation of these dyes, we were further able to perform time-lapse dSTORM imaging of directly labeled DNA.

Theoretically, by choosing an appropriate reducing–oxidizing system, one can achieve the controllable reversible photoswitching required for the dSTORM of nearly any cyanine derivative. Several cyanine-based dyes have already been used in dSTORM imaging.[17, 18] Typically, enzymatic oxygen-scavenging buffers are used to prevent the irreversible photobleaching of dyes, and mercaptoethylamine (MEA) is used as a reducing

agent to induce photoswitching or photoblinking.[19] MEA is responsible for converting the dye into long-lived, dark, nonfluorescent states from which single molecules can spontaneously recover to the ground state upon interaction with residual oxygen; this is the photochemical basis of dSTORM. Buffer conditions determine oxygen concentration and reduction rate, and are therefore important for optimizing photoswitching rates.

To perform live-cell imaging, we avoided adding the potentially toxic thiol reducing agents, such as MEA, that are commonly used to induce photoblinking.[20] We tested buffer conditions that have worked for live-cell dSTORM in the past for other dyes. In phosphate-buffered saline (PBS) alone, we observed rapid photobleaching of Picogreen with no recovery (Figure 1 A). When using a buffer containing an oxygen-scavenging (OS) system composed of 10% glucose, 0.5 mg mL^{-1} glucose oxidase, and 40 µg mL^{-1} catalase, the fluorescence intensity over time showed a much slower decay. Thus, enzymatic removal of oxygen indeed helps to avoid photobleaching of the dye. However, it was not sufficient to induce the single molecule blinking required in dSTORM. To improve the recovery and photoblinking of Picogreen, we applied ascorbic acid (AA) as a reducing agent and the OS to reduce irreversible photobleaching.[21] We found that 1 mM ascorbic acid com-
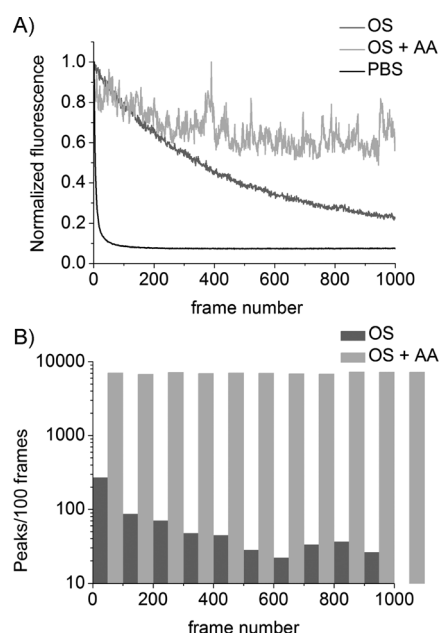

Figure 1. Picogreen photoswitching dynamics. U2OS cells labeled with Picogreen and in different imaging buffers were imaged by using a 488 nm laser with an excitation power of ca. 1 kW cm^{-2} in the focal plane. A) Fluorescence decay curves for a 300×300 nm square region of interest. B) Time dependence of the number of localized peaks averaged over multiple frames (note the logarithmic scale).

[a] A. Benke, Prof. S. Manley
Laboratory of Experimental Biophysics
École Polytechnique Fédérale de Lausanne
1005 Lausanne (Switzerland)
E-mail: suliana.manley@epfl.ch

bined with this OS system in Leibowitz medium at pH 7.2 allowed rapid and reversible photoswitching (Figure 1 A). In this medium, a large number of molecules could be localized in each raw image, over thousands of images, as shown in Figure 1 B.

dSTORM of living cells requires fast acquisition. This in turn necessitates a high number of peaks per frame to satisfy the Nyquist criterion for determining object structure while maintaining nanometer molecular localization.[22] This is particularly true for DNA, with its intricate and dense structure. In our optimized medium, individual raw images show a large number of peaks, suitable for live dSTORM imaging (Figure 2). We ob-

and efficient photoswitching of Picogreen enabled a resolution of 70 nm, as measured by the full width half maximum (Figure 3 C). This is better by a factor of approximately 5 than can be obtained with conventional epi-fluorescence imaging.

One goal of live-cell imaging is to monitor changes in cellular structures over time. Many dyes do not have good enough recovery from photobleaching to give a sustained signal over many images. We tested the possibility of time-lapse dSTORM by allowing the Picogreen fluorophores 10 min to recover from longer-lived dark states before acquiring the next stack of raw images. The individual stacks were used to construct a series of dSTORM images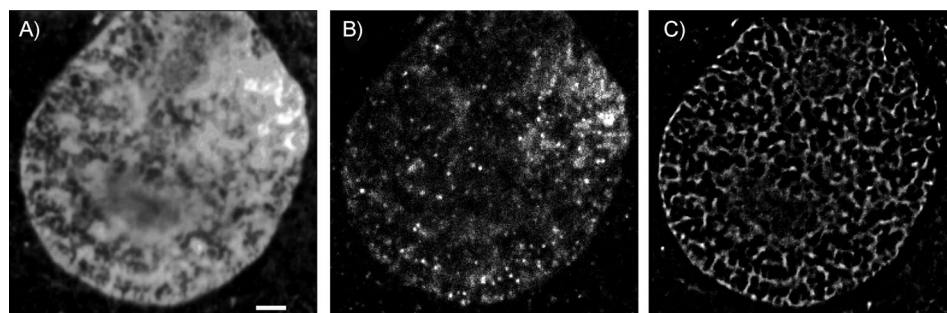 (Figure 4 A), thus demonstrating that it is possible to monitor the sub-diffraction-limited organization of DNA in individual cells over time. The total number of molecules in each dSTORM image was quite constant, varying only by ~10–20%. The number of molecules per raw image showed more fluctuations, probably due to cellular processes (Figure 4 B). The dynamics of DNA fibers can be more clearly seen by looking at the differences between consecutive dSTORM images (Figure 4 C).

Commercially available, DNA-

Figure 2. Live-cell dSTORM of cellular DNA based on direct DNA labeling with Picogreen. A) Wide-field diffraction-limited image, B) single raw dSTORM frame demonstrating Picogreen single-molecule photoswitching—seen as bright spots—and C) final dSTORM image reconstructed from 8000 frames. Scale bar represents 2.5 μm.

tained 3500 peaks per μm² for a stack of 8000 raw images, acquired at 30 ms per frame—a sufficiently high density of well-localized molecules to reconstruct super-resolution structure (Figure 2). The organization of the DNA revealed by the live dSTORM image would not be possible to deduce from the epi-fluorescence image. Due to the improved resolution and coincident axial sectioning from dSTORM, continuous fibers of DNA could be resolved.

We also observed a small pool of extranuclear cellular DNA representing mitochondrial nucleoids. To quantify the resolution achievable with Picogreen, we also visualized these individual mitochondrial DNA nucleoids in living cells (Figure 3 A). Nucleoids appear as bright punctate structures along elongated mitochondria, the size of which is greatly reduced in dSTORM imaging (Figure 3 B). The brightness, high specificity,

specific cyanine dyes can be used for live-cell dSTORM, and even time-lapse dSTORM imaging, thereby giving insight into the dynamics of DNA organization at unprecedented resolution. This provides an advantageous approach to studying processes related to DNA dynamic structural rearrangements such as those occurring during cell division or in response to stress. Furthermore, this represents a complementary tool to those previously developed[12,23] and permits combined DNA and protein super-resolution imaging. Potential applications include the study of chromatin reorganization and the dependence of DNA organization on gene expression in high-transcription versus silent regions. We further suggest that other commercially available affinity dyes can be used to target cellular structures and organelles directly for super-resolution imaging.
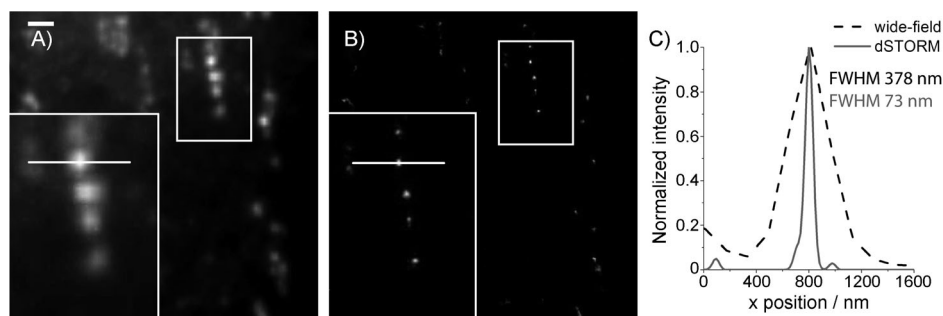
Experimental Section

Cell culture: U2OS cells were cultured in DMEM Glutamax-I medium (Gibco/Invitrogen) supplemented with 10% fetal bovine serum FBS (Invitrogen) under 5% CO_2 at 37 °C. Cells were normally split every 2–3 days depending on their confluence.

Cell labeling: Cells were plated 24 h before labeling on 25 mm glass coverslips (ca. 75 000 cells

Figure 3. A) Wide-field and B) dSTORM images of mitochondrial DNA. Scale bars represent 1 μm. C) Line-intensity profiles (from lines in A and B) and calculated full width half maxima (FWHM) of corresponding structures.
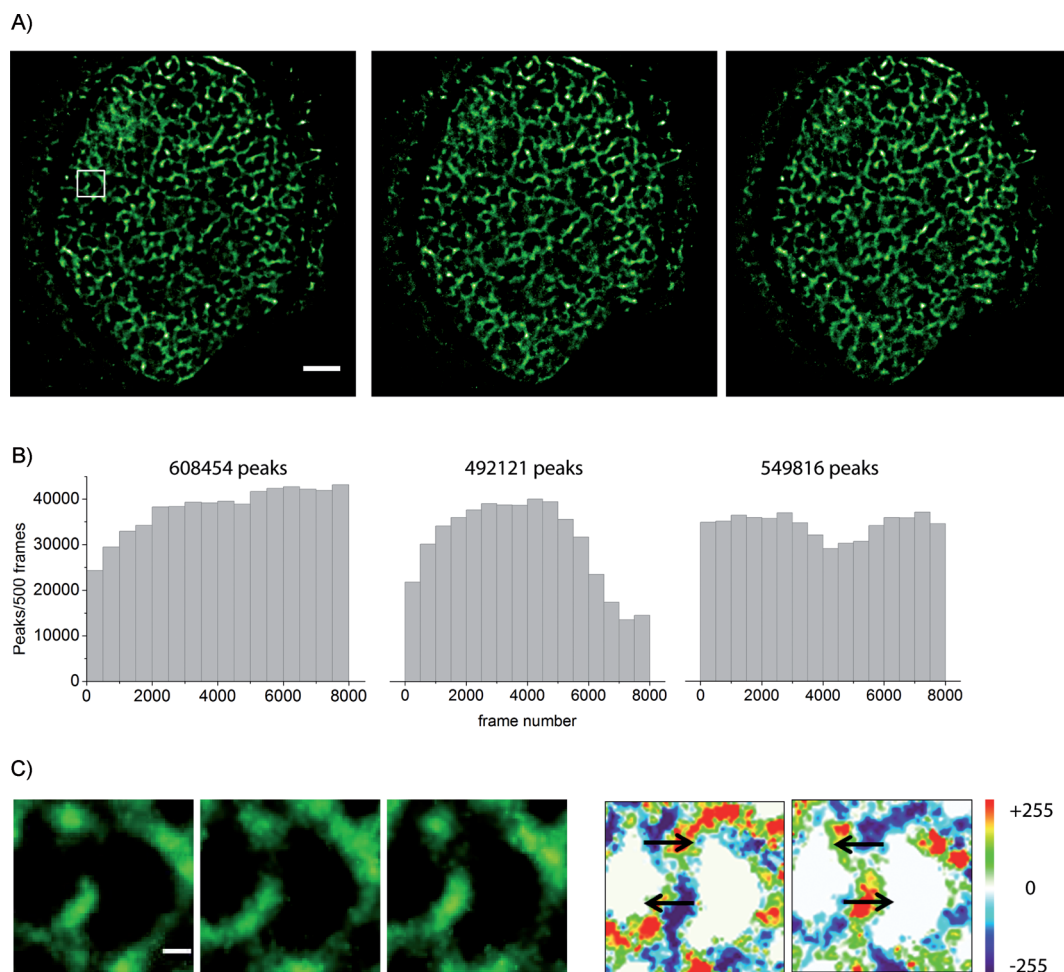
Figure 4. Time-lapse dSTORM. A) Three consecutive dSTORM images (8000 frames each) with 10 min interim pause. Scale bar represents 2.5 μm. B) Time dependence of the number of peaks for each raw image stack. The total number of localized molecules for each dSTORM image is indicated. Note that the variation in number of molecules across images is small. C) Zoom of dSTORM images (left) showing local rearrangements, highlighted by consecutive image subtraction (right). Subtracted dSTORM images demonstrate chromatin fiber subdiffractional dynamics. Arrows indicate the direction of motion. Scale bar represents 200 nm.

per coverslip). On the day of the experiment, cells were washed in PBS (Sigma) and labeled with Picogreen (1:500 dilution from original stock of Quant-iT PicoGreen; Invitrogen) in DMEM without Phenol Red (Gibco/Invitrogen) and incubated for 15 min at 37 °C. Then cells were washed again, and prewarmed imaging buffer was added (1 mм ascorbic acid, 10 % glucose, 0.5 mg mL^{-1} glucose oxidase, 40 μg mL^{-1} catalase (all Sigma) in Leibowitz medium (Gibco/Invitrogen), pH 7.2).

Live-cell dSTORM imaging: Wide-field and dSTORM imaging was performed on an inverted microscope (Axio Observer.D1; Zeiss) equipped with a TIRF module. A 488 nm laser (Sapphire 488–50, Coherent, Santa Clara, CA) used to excite Picogreen was focused on the back focal plane of the oil-immersion objective (α Plan-Apochromat, 100×, NA = 1.46; Zeiss). Fluorescent light collected by this objective then was projected onto an EMCCD camera (iXon+; Andor, Belfast, UK). Additional lenses resulted in a final pixel size of 100 nm. To minimize drift, the objective was mounted on a piezo-driven objective scanner (N-725, PI, Karlsruhe, Germany) and samples were mounted into a stainless-steel holder bolted onto a motorized stage (ProScan III; Prior, Cambridge, UK). Typically, we acquired 2000–8000 images (30 ms per frame) with a laser excitation intensity of 1–5 kW cm^{-2} for a total acquisition time of 1–4 min for a single dSTORM image.

Data analysis: Raw data were analyzed by using Peakselector software provided by Harald Hess (previously described in ref. [8]). Peaks were selected based on peak width, number of photons, and localization precision. Peaks with a width between 120 and 400 nm, 100–3000 photons, and a localization precision of less than 50 nm were considered as good single-molecule localizations. A standard grouping procedure was also applied to group molecules appearing in consecutive frames. dSTORM images were rendered as the sum of superimposed filtered peaks with a width corresponding to their empirically determined localization precision.

[1] E. Betzig, G. H. Patterson, R. Sougrat, O. W. Lindwasser, S. Olenych, J. S. Bonifacino, M. W. Davidson, J. Lippincott-Schwartz, H. F. Hess, *Science* **2006**, *313*, 1642–1645.

[2] S. T. Hess, T. P. K. Girirajan, M. D. Mason, *Biophys. J.* **2006**, *91*, 4258–4272.

[3] M. J. Rust, M. Bates, X. Zhuang, *Nat. Methods* **2006**, *3*, 793–795.

[4] M. Hofmann, C. Eggeling, S. Jakobs, S. W. Hell, *Proc. Natl. Acad. Sci. USA* **2005**, *102*, 17565–17569.

[5] R. E. Thompson, D. R. Larson, W. W. Webb, *Biophys. J.* **2002**, *82*, 2775–2783.

[6] A. Yildiz, J. N. Forkey, S. A. McKinney, T. Ha, Y. E. Goldman, P. R. Selvin, *Science* **2003**, *300*, 2061–2065.

[7] B. Huang, W. Wang, M. Bates, X. Zhuang, *Science* **2008**, *319*, 810–813.

[8] G. Shtengel, J. A. Galbraith, C. G. Galbraith, J. Lippincott-Schwartz, J. M. Gillette, S. Manley, R. Sougrat, C. M. Waterman, P. Kanchanawong, M. W. Davidson, R. D. Fetter, H. F. Hess, *Proc. Natl. Acad. Sci. USA* **2009**, *106*, 3125–3130.

[9] G. Patterson, M. Davidson, S. Manley, J. Lippincott-Schwartz, *Annu. Rev. Phys. Chem.* **2010**, *61*, 345–367.

[10] M. Fernandez-Suarez, A. Y. Ting, *Nat. Rev. Mol. Cell Biol.* **2008**, *9*, 929–943.

[11] M. Heilemann, S. van de Linde, A. Mukherjee, M. Sauer, *Angew. Chem.* **2009**, *121*, 7036–7041; *Angew. Chem. Int. Ed.* **2009**, *48*, 6903–6908.

[12] R. Wombacher, M. Heidbreder, S. van de Linde, M. P. Sheetz, M. Heilemann, V. W. Cornish, M. Sauer, *Nat. Methods* **2010**, *7*, 717–719.

[13] T. Klein, A. Löschberger, S. Proppert, S. Wolter, S. van de Linde, M. Sauer, *Nat. Methods* **2011**, *8*, 7–9.

[14] L. W. Miller, Y. Cai, M. P. Sheetz, V. W. Cornish, *Nat. Methods* **2005**, *2*, 255–257.

[15] A. Keppler, S. Gendreizig, T. Gronemeyer, H. Pick, H. Vogel, K. Johnsson, *Nat. Biotechnol.* **2003**, *21*, 86–89.

[16] C. Flors, C. N. J. Ravarani, D. T. F. Dryden, *ChemPhysChem* **2009**, *10*, 2201–2204.

[17] M. Heilemann, S. van de Linde, M. Schöttpelz, R. Kasper, B. Seefeldt, A. Mukherjee, P. Tinnefeld, M. Sauer, *Angew. Chem.* **2008**, *120*, 6266–6271; *Angew. Chem. Int. Ed.* **2008**, *47*, 6172–6176.

[18] S. van de Linde, M. Sauer, M. Heilemann, *J. Struct. Biol.* **2008**, *164*, 250–254.

[19] S. van de Linde, A. Löschberger, T. Klein, M. Heidbreder, S. Wolter, M. Heilemann, M. Sauer, *Nat. Protoc.* **2011**, *6*, 991–1009.

[20] S. van de Linde, R. Kasper, M. Heilemann, M. Sauer, *Appl. Phys. B Lasers Opt.* **2008**, *93*, 725–731.

[21] C. Steinhauer, C. Forthmann, J. Vogelsang, P. Tinnefeld, *J. Am. Chem. Soc.* **2008**, *130*, 16840–16841.

[22] H. Shroff, C. G. Galbraith, J. A. Galbraith, E. Betzig, *Nat. Methods* **2008**, *5*, 417–423.

[23] S. A. Jones, S.-H. Shim, J. He, X. Zhuang, *Nat. Methods* **2011**, *8*, 499–505.